Electronic Supplementary Material (ESI) for Sustainable Energy & Fuels.

Supplementary Material for

Boosting pseudocapacitive charge storage in in-situ functionalized carbons with high surface area for high-energy asymmetric supercapacitors

Hao Zhang, [‡a] Mingjie Lu, [‡a] Huanlei Wang, [*a] Yan Lyu, [a] Dong Li, [a] Shijiao Sun, [b] Jing Shi, [a] and Wei Liu [a]

[a] *School of Materials Science and Engineering, Ocean University of China, Qingdao 266100, People's Republic of China*

[b] *College of Materials Science and Engineering, Nanjing Tech University, Nanjing 210009, People's Republic of China*

‡ These authors contribute equally to this work.

* Corresponding author.

E-mail address: huanleiwang@ouc.edu.cn; huanleiwang@gmail.com (H. Wang).

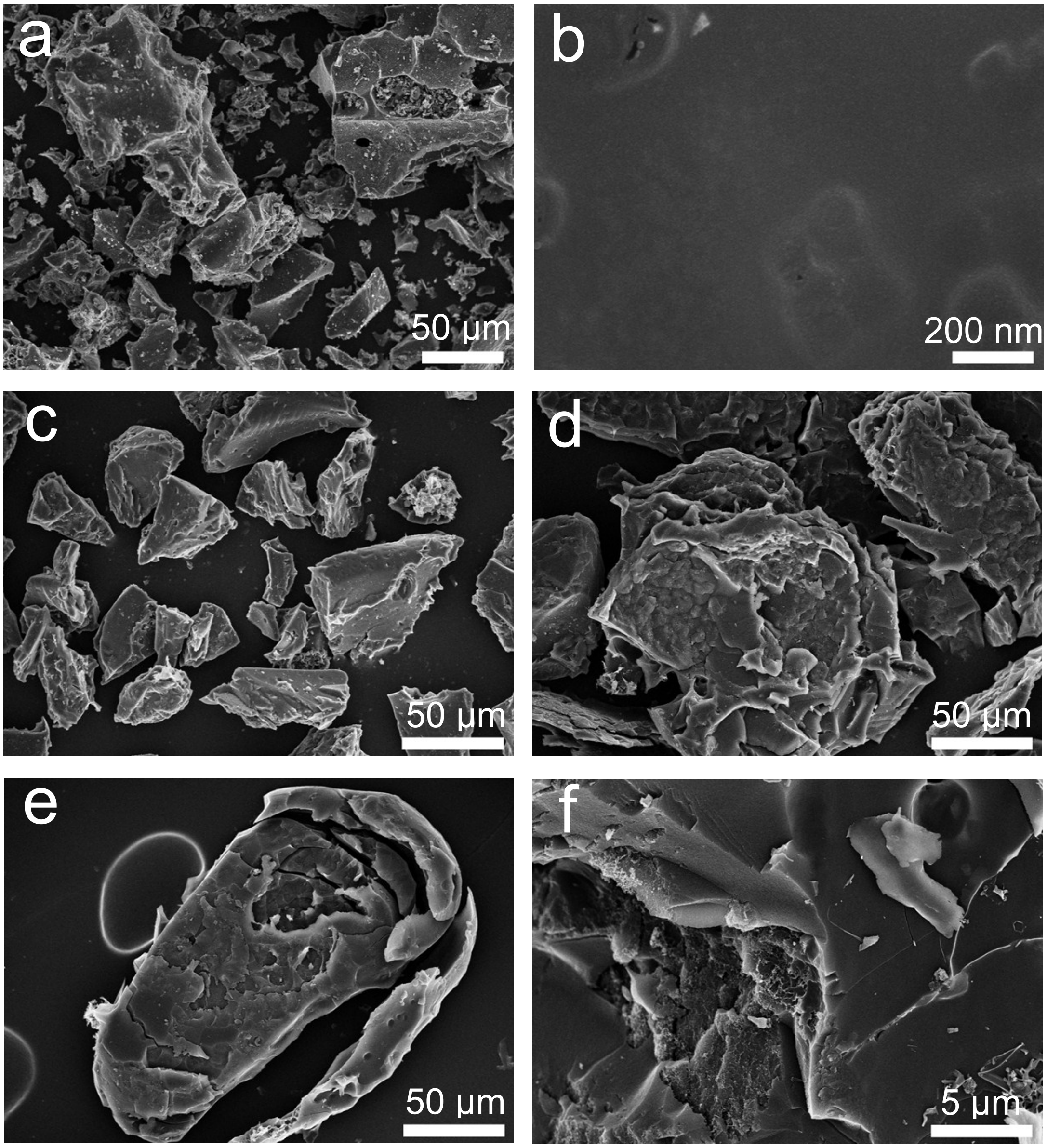

Fig. S1 SEM images of (a) (b) PC, (c) HFJDAC-500, (d) HFJDAC-600, (e) HFJDAC-700, and (f) HFJDAC-800.

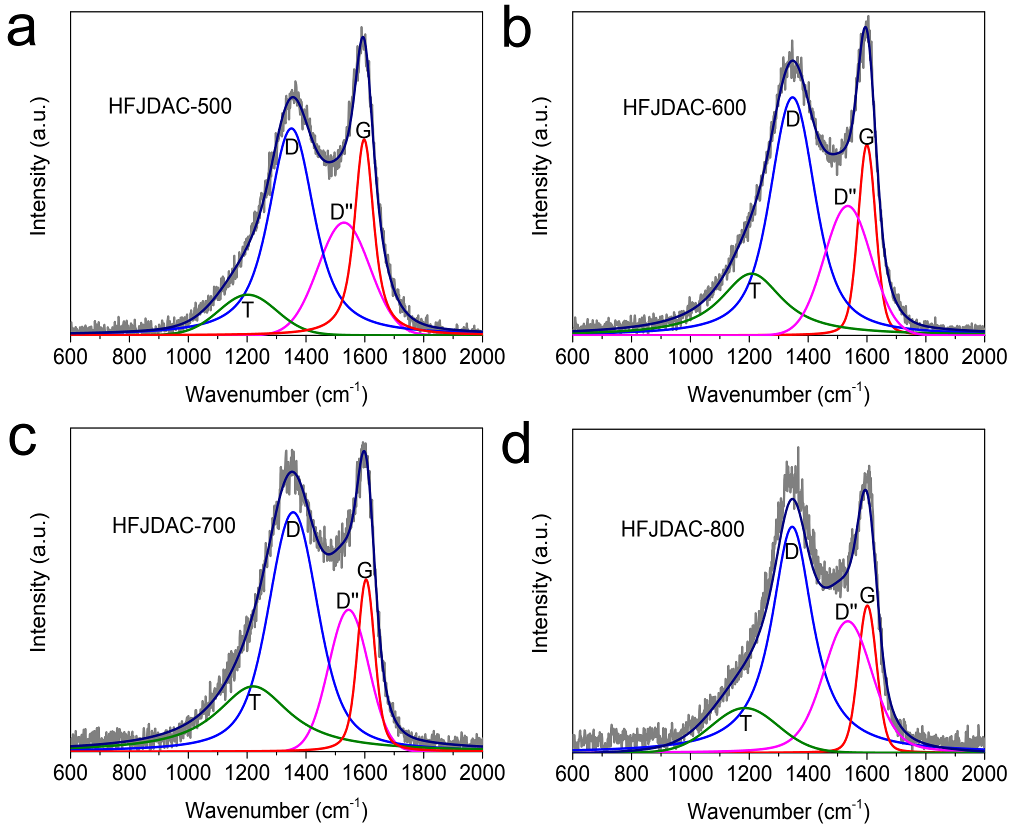

Fig. S2 Raman spectra of HFJDAC samples.

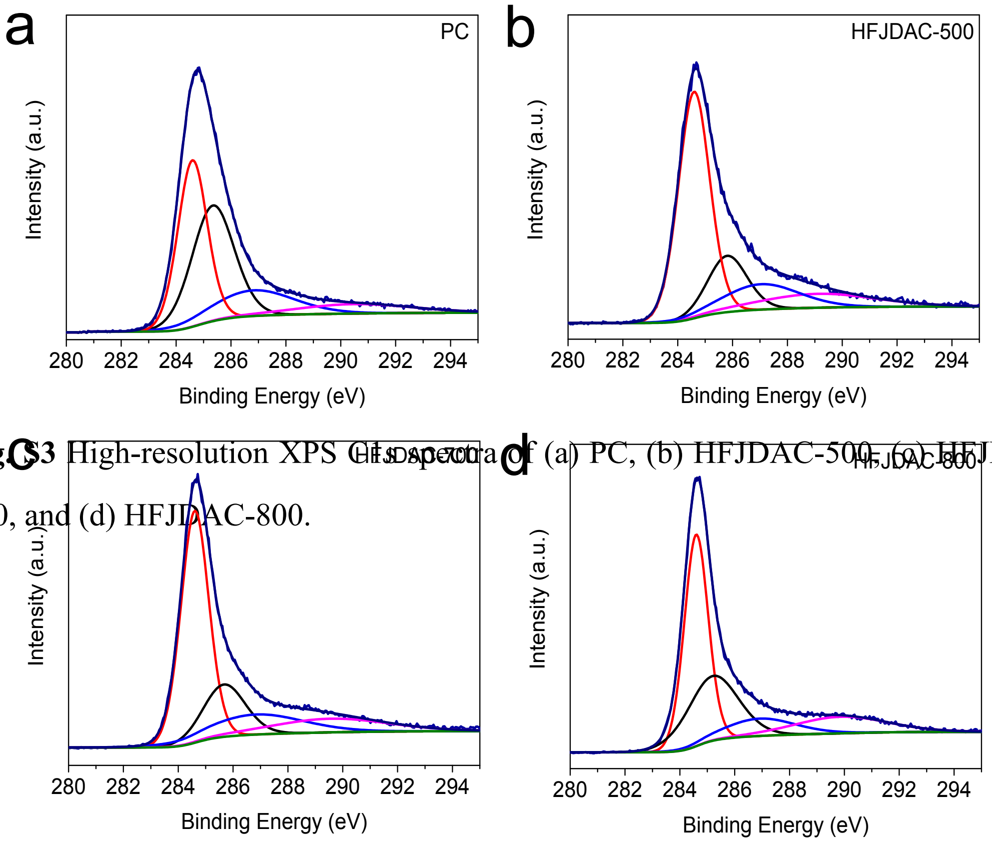

Fig. S3 High-resolution XPS C1s spectra of (a) PC, (b) HFJDAC-500, (c) HFJDAC-700, and (d) HFJDAC-800.

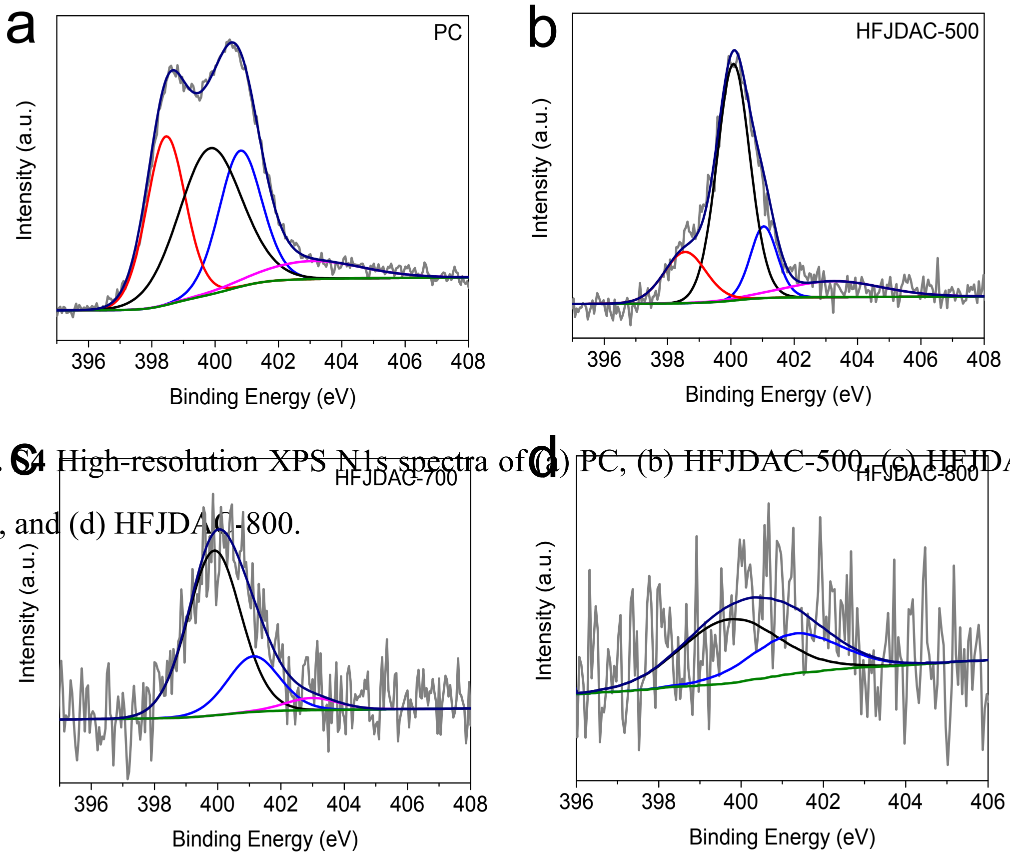

Fig. S4 High-resolution XPS N1s spectra of (a) PC, (b) HFJDAC-500, (c) HFJDAC-700, and (d) HFJDAC-800.

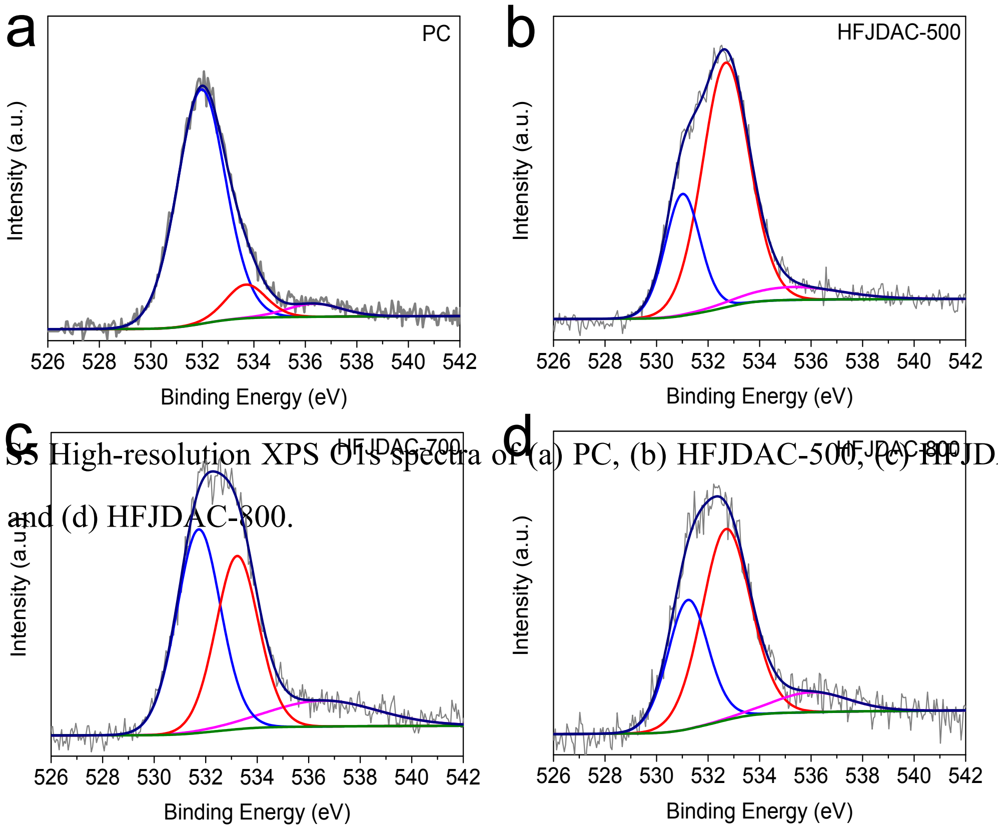

Fig. S5 High-resolution XPS O1s spectra of (a) PC, (b) HFJDAC-500, (c) HFJDAC-700, and (d) HFJDAC-800.

Table S1 Relative surface concentrations (%) of nitrogen and oxygen species obtained by fitting N1s and O1s core level XPS spectra.

Sample	N-6	N-5	N-Q	N-X	O-I	O-II	O-III
PC	28.06	39.34	24.89	7.71	84.56	10.10	5.34
HFJDAC-500	16.05	58.12	14.39	11.44	25.07	67.57	7.36
HFJDAC-600	23.73	48.10	16.94	11.23	23.04	65.01	11.95
HFJDAC-700	0	71.25	23.56	5.19	46.66	38.64	14.70
HFJDAC-800	0	63.80	36.20	0	32.68	58.13	9.19

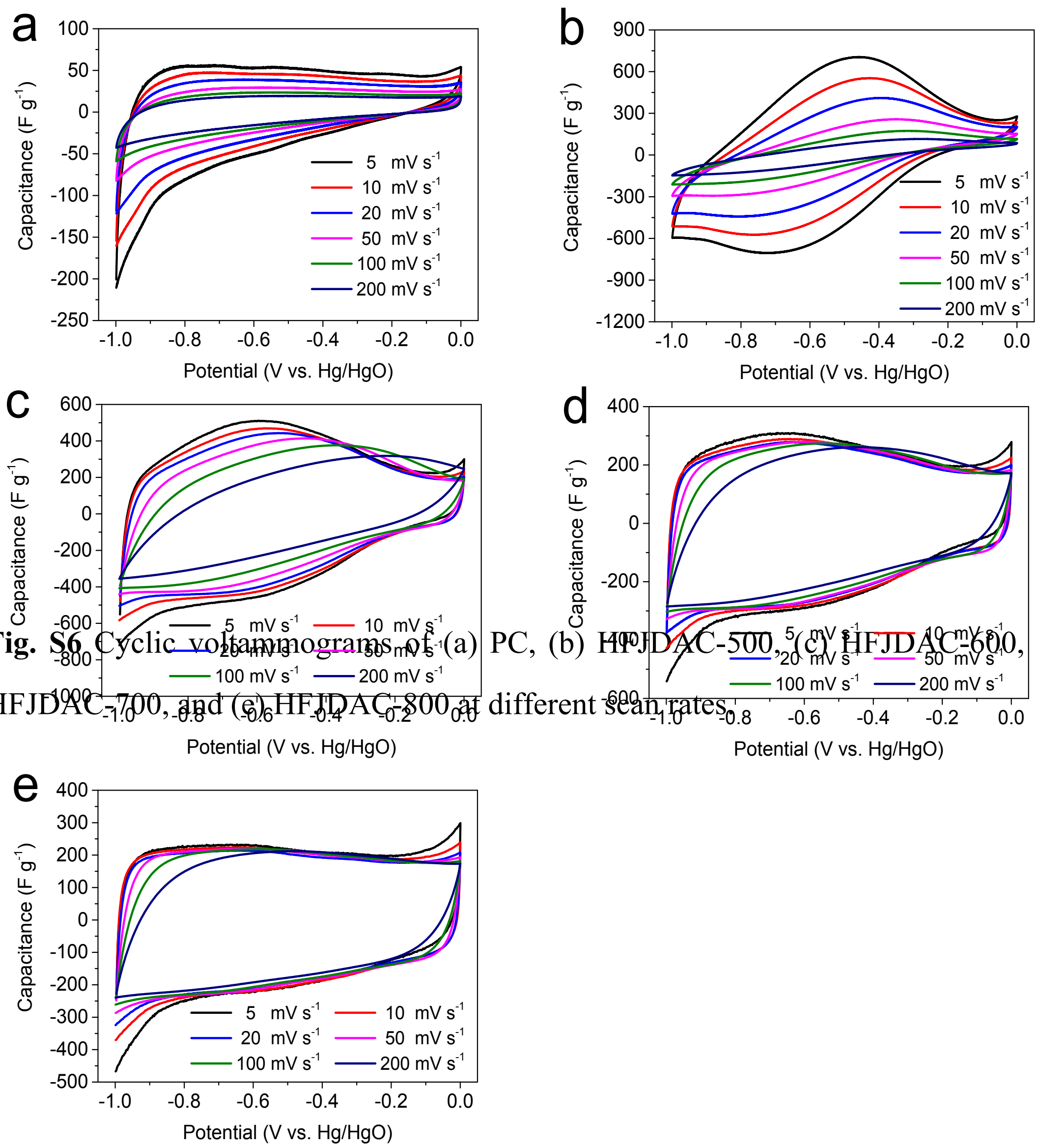

Fig. S6 Cyclic voltammograms of (a) PC, (b) HFJDAC-500, (c) HFJDAC-600, (d) HFJDAC-700, and (e) HFJDAC-800 at different scan rates.

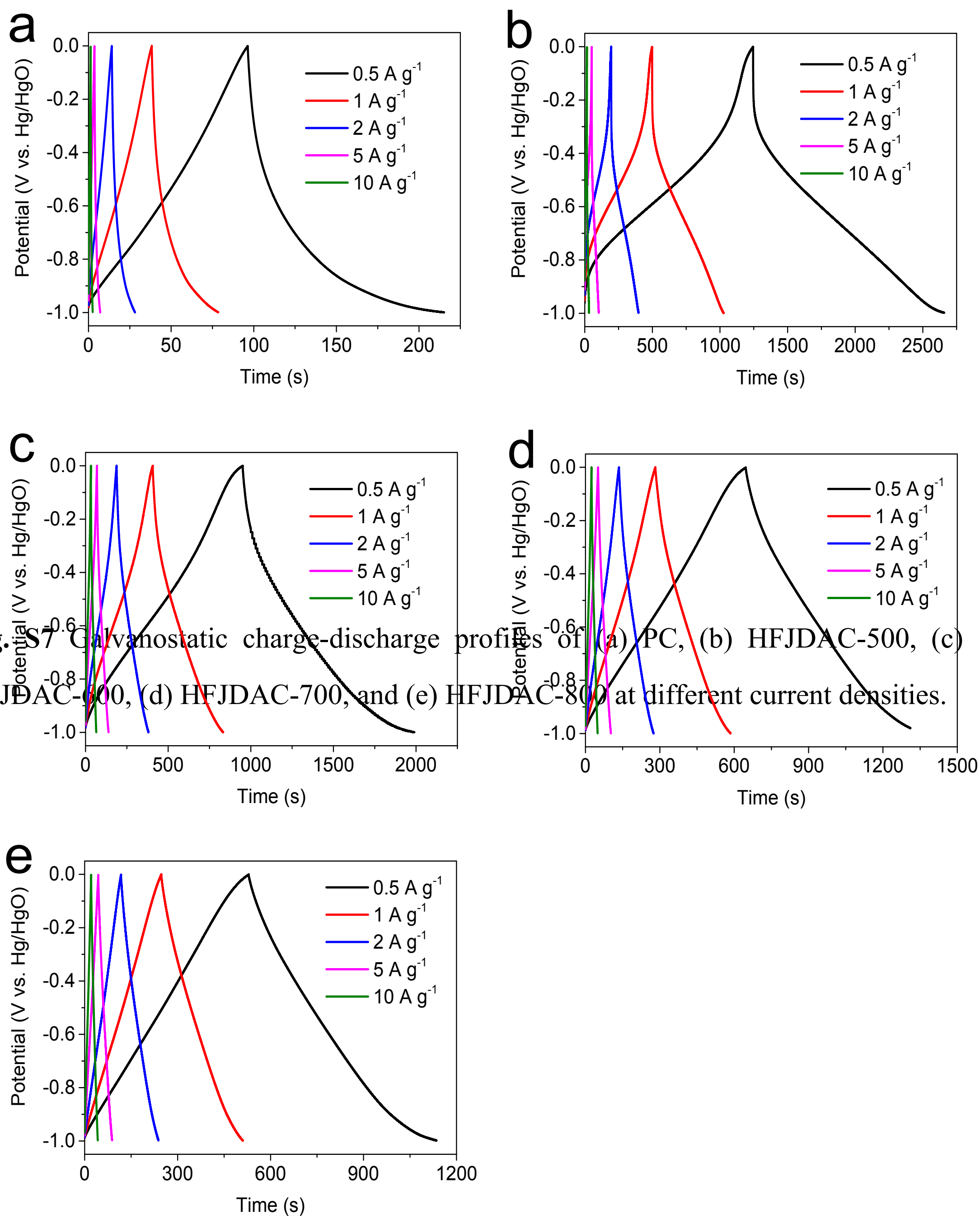

Fig. S7 Galvanostatic charge-discharge profiles of (a) PC, (b) HFJDAC-500, (c) HFJDAC-600, (d) HFJDAC-700, and (e) HFJDAC-800 at different current densities.

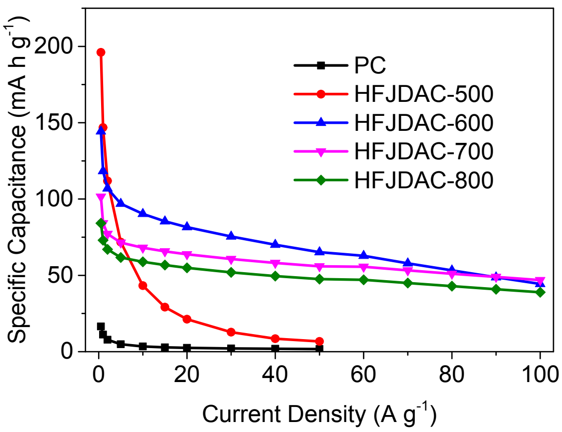

Fig. S8 Specific capacitances (mA h g^{-1}) at different current densities.

Table S2 Specific capacitance of HFJDAC-600 versus recently published state-of-the-art carbons, all tested in a three-electrode system.

Carbon Type	**Capacitance ($F\ g^{-1}$)**	**Current Density/ Scan Rate**	**Electrolyte**	**Reference**
HFJDAC-600	430	1 A g^{-1}	2 M KOH	This work
Multi-heteroatom self-doped porous carbon	385/346	1 A g^{-1}	1 M H_2SO_4/ 1 M KOH	1
Porous carbon nanosheets	470	1 A g^{-1}	6 M KOH	2
Doped carbon nanoflakes	474	0.5 A g^{-1}	2 M KOH	3
Peanut-shell-like porous carbon	356	1 A g^{-1}	1 M H_2SO_4	4
Functionalized three-dimensional grapheme networks	442.8	2 mV s^{-1}	6 M KOH	5
Nitrogen-doped carbon networks	296	2 mV s^{-1}	6 M KOH	6

Biomass-derived 3D hierarchical porous carbon	356	1 A g^{-1}	6 M KOH	7
Sodium glutamate derived micro/mesoporous carbon	406	0.5 A g^{-1}	6 M KOH	8
Nitrogen-enriched hierarchically porous carbons	641.6	1 A g^{-1}	6 M KOH	9
Honeycomb-like porous carbon	342	0.2 A g^{-1}	6 M KOH	10
Biomass-derived carbon fiber aerogel	283	1 A g^{-1}	6 M KOH	11
Nitrogen and sulfur co-doped porous carbon nanosheets	298	0.5 A g^{-1}	6 M KOH	12
Nitrogen-doped porous carbon superstructures	364	0.6 A g^{-1}	6 M KOH	13
Human hair-derived carbon flakes	340	1 A g^{-1}	6 M KOH	14
Stacked layer-like porous carbon	366	1 A g^{-1}	6 M KOH	15
Hierarchically porous and heteroatom doped carbon	286.6	0.5 A g^{-1}	6 M KOH	16
Hierarchical carbon	401	5 A g^{-1}	1 M H_2SO_4	17
Heteroatom-containing porous carbons	287	1 A g^{-1}	6 M KOH	18
Highly functionalized activated carbons	481/445	0.5 A g^{-1}	1 M H_2SO_4/ 1 M KOH	19
Nitrogen-doped porous carbon buildings	347	1 A g^{-1}	6 M KOH	20
Nitrogen-doped hierarchical micro/mesoporous carbon nets	537.3	0.5 A g^{-1}	0.5M H_2SO_4	21
Hierarchically porous nitrogen-doped carbon	383	1 A g^{-1}	1 M H_2SO_4	22
Interconnected honeycomb-like porous carbon	493	0.2 A g^{-1}	2 M H_2SO_4	23
Hollow activated carbon nanomesh	314.6	1 A g^{-1}	6 M KOH	24
Egg protein derived carbon	482	0.1 A g^{-1}	1 M H_2SO_4	25
Coca Cola® derived carbon	352.7	1 A g^{-1}	6 M KOH	26
Three-dimensional laminated porous carbon network	337.4	0.5 A g^{-1}	6 M KOH	27
Porous carbon	350	1 A g^{-1}	6 M KOH	28
Biomass-derived hierarchical porous carbon	336	1 A g^{-1}	6 M KOH	29
Nitrogen-doped porous carbon	429	1 A g^{-1}	6 M KOH	30

Pine cone biochar carbon	361	10 mV s^{-1}	1 M H_2SO_4	31
Black liquor-derived porous carbon	337	0.5 A g^{-1}	6 M KOH	32
Biomass-derived interconnected carbon	532.5/350	1 A g^{-1}	1 M H_2SO_4/ 1 M KOH	33
Hierarchical porous graphitic carbons	274	1 A g^{-1}	6 M KOH	34
Biomass organs pyrolyzed carbon	174	5 mV s^{-1}	6 M KOH	35
Nitrogen-doped porous carbons	267	1 A g^{-1}	2 M KOH	36

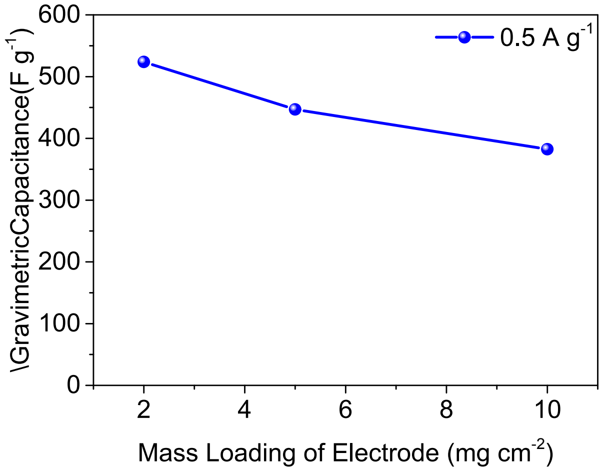

Fig. S9 Comparison of the gravimetric capacitance of the HFJDAC-600 electrodes at different mass loading tested in a 2 M KOH electrolyte at a current density of 0.5 A g^{-1} between -1 and 0 V.

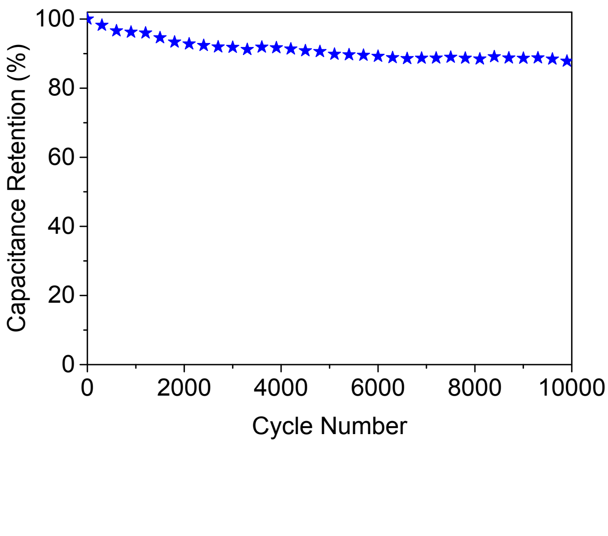

Fig. S10 Cycling stability of HFJDAC-600 tested at 20 A g^{-1} for 10,000 cycles.

Trasatti Method Analysis

We select Trasatti method to assess the capacitance contribution of jelly fish derived carbons.[37] The main formulas are as follows:

The gravimetric specific capacitance of electrode in three-electrode configuration was calculated according to the CV curves at different scan rates based on the following equation:

$$C = (\int I \, dV) / (m \cdot v \cdot V)$$

where C (F g^{-1}) indicates the gravimetric capacitance, I (A) indicates the current density, m (g) indicates the mass of the active material in the electrode, v (V s^{-1}) indicates the scan rate, and V (V) indicates the voltage window.

The maximum gravimetric capacitance (C_m) can be calculated based on the following equation:

$$C^{-1} = constant \cdot v^{1/2} + C_m^{-1}$$

where C denotes the calculated gravimetric capacitance, v denotes the scan rate, and C_m denotes the maximum gravimetric capacitance. The "maximum gravimetric capacitance (C_m)" is equal to the total of electrical double layer capacitance and pseudocapacitance. C_m equals the reciprocal of the y-intercept of the C^{-1} vs. $v^{1/2}$ plot (Fig. S11, left columns).

Plotting the calculated gravimetric capacitances (C) against the reciprocal of square root of scan rates ($v^{-1/2}$) gives the opportunity to calculate the maximum electrical double layer capacitance (C_e) based on the following equation:

$$C = constant \cdot v^{-1/2} + C_e$$

where C represents the calculated gravimetric capacitance, v represents the scan rate, and C_e represents the maximum electrical double layer capacitance. Linear fit the plot and extrapolate the fitting line to y-axis gives the C_e (Fig. S11, right columns). Subtraction of C_e from C_m yields the maximum pseudocapacitance (C_p).

Finally, the capacitance contribution from electrical double layer capacitance and pseudocapacitance can be calculated as follows:

$$C_e\% = (C_e / C_m) \cdot 100\%$$

$$C_p\% = (C_p / C_m)\cdot 100\%$$

where $C_e\%$ is the capacitance percentage of electrical double layer capacitance and $C_p\%$ is the capacitance percentage of pseudocapacitance.

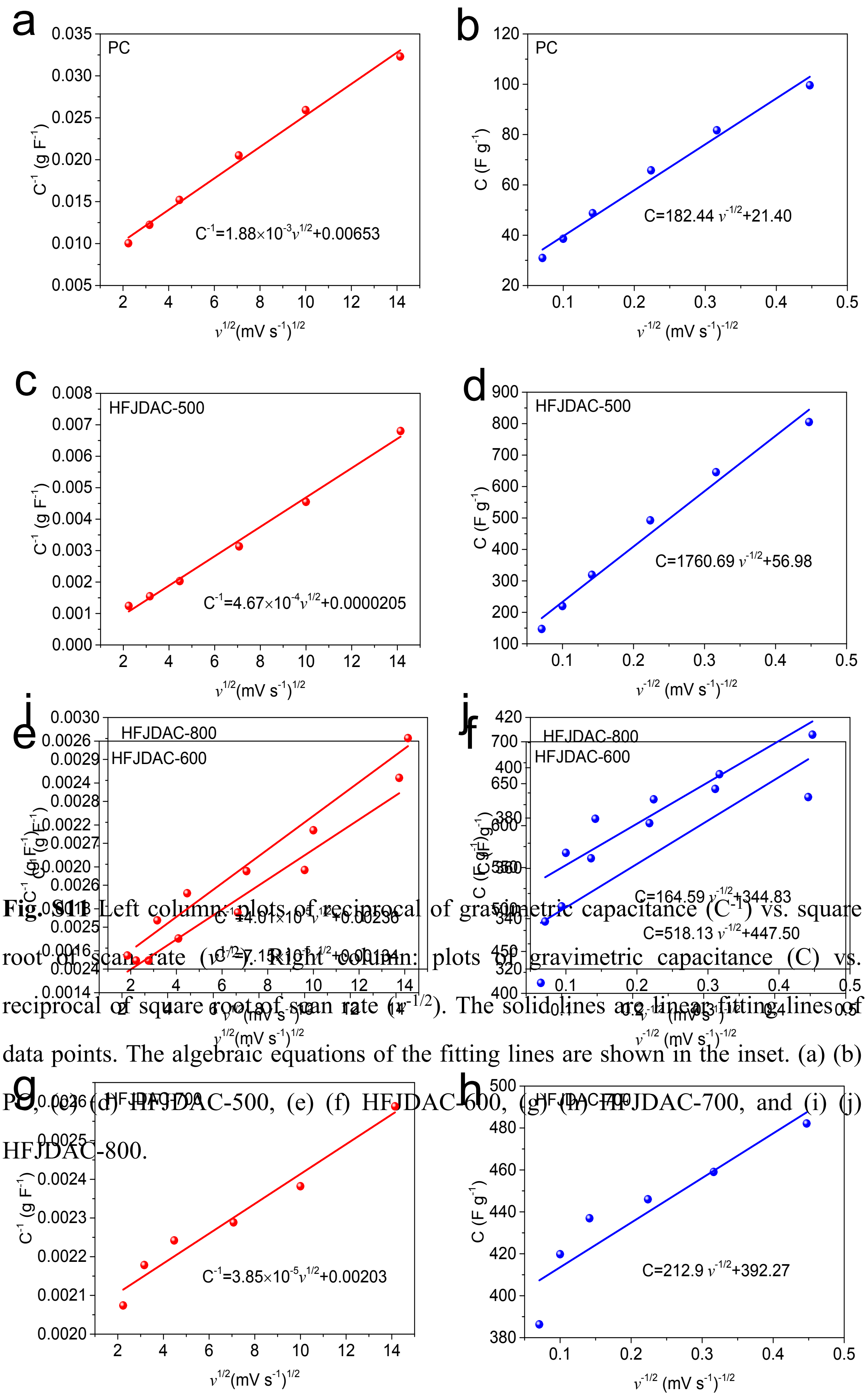

Fig. S11 Left column: plots of reciprocal of gravimetric capacitance (C^{-1}) vs. square root of scan rate ($v^{1/2}$). Right column: plots of gravimetric capacitance (C) vs. reciprocal of square root of scan rate ($v^{-1/2}$). The solid lines are linear fitting lines of data points. The algebraic equations of the fitting lines are shown in the inset. (a) (b) PC, (c) (d) HFJDAC-500, (e) (f) HFJDAC-600, (g) (h) HFJDAC-700, and (i) (j) HFJDAC-800.

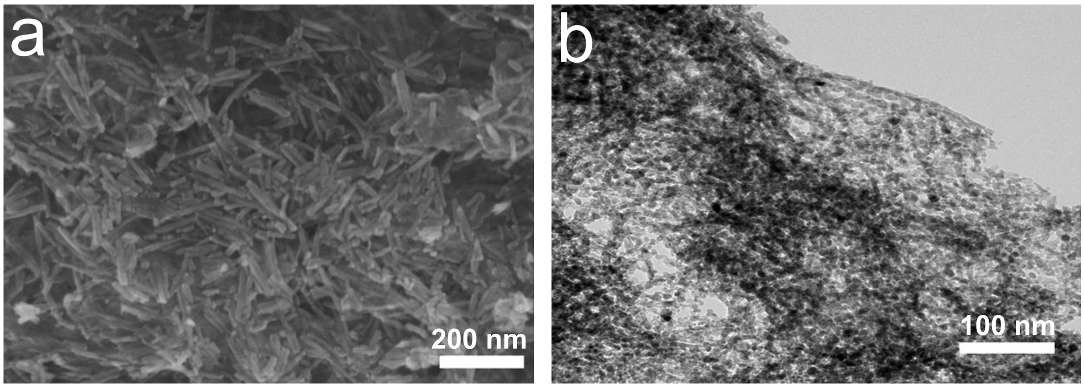

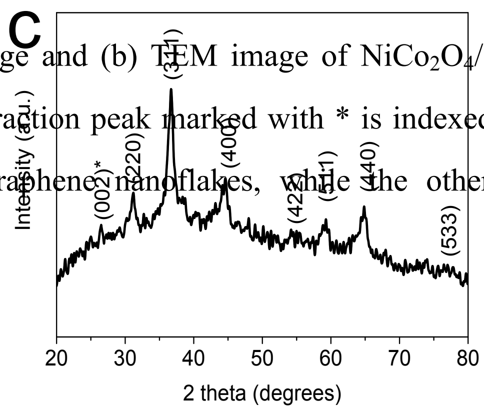

Fig. S12 (a) SEM image and (b) TEM image of $NiCo_2O_4$/GR, (c) XRD pattern of $NiCo_2O_4$/GR, the diffraction peak marked with * is indexed as (002) graphitic peak associated with the graphene nanoflakes, while the other peaks are indexed as equilibrium $NiCo_2O_4$.

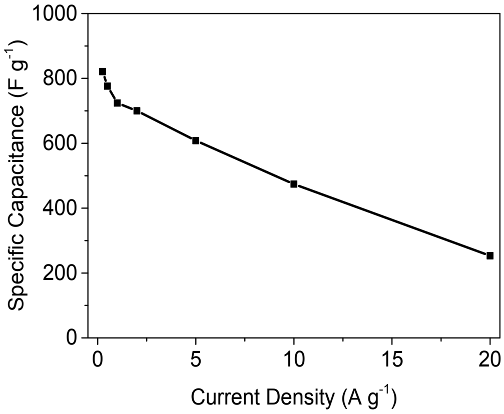

Fig. S13 Specific capacitances of $NiCo_2O_4$/GR at different current densities in a three-electrode system tested in 2M KOH.

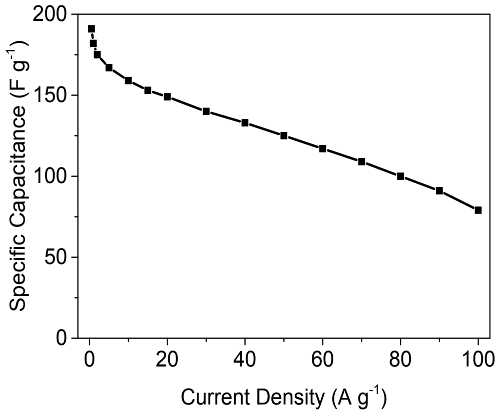

Fig. S14 Specific capacitances of AC at different current densities in a three-electrode system tested in 2M KOH.

Table S3 Comparison of $NiCo_2O_4$/GR//HFJDAC-600 with previously reported nickel/cobalt based asymmetric cells.

Sample	Specific capacity ($F\ g^{-1}$)		Energy-power density	Reference
	Positive	Negative		
$NiCo_2O_4$/GR//HFJDAC-600	700	389	43.4 $W\ h\ kg^{-1}$ at 187 $W\ kg^{-1}$ 13.3 $W\ h\ kg^{-1}$ at 16.4 $kW\ kg^{-1}$	This work
$Ni_xCo_{3-x}O_4$//AC	1479	187	37.4 $W\ h\ kg^{-1}$ at 163 $W\ kg^{-1}$ 20.9 $W\ h\ kg^{-1}$ at 4.1 $kW\ kg^{-1}$	38
$NiCo_2O_4$@MnO_2//AC	913.6	-	37.8 $W\ h\ kg^{-1}$ at 187.5 $W\ kg^{-1}$ 13.3 $W\ h\ kg^{-1}$ at 7.5 $kW\ kg^{-1}$	39
CQDs/$NiCo_2O_4$//AC	856	180	27.8 $W\ h\ kg^{-1}$ at 128 $W\ kg^{-1}$ 13.1 $W\ h\ kg^{-1}$ at 10.2 $kW\ kg^{-1}$	40
$NiCo_2S_4$//G/CS	1036	-	42.3 $W\ h\ kg^{-1}$ at 476 $W\ kg^{-1}$ 22.9 $W\ h\ kg^{-1}$ at 10.2 $kW\ kg^{-1}$	41
$Ni(OH)_2$/CNT//AC	3300	120	50.6 $W\ h\ kg^{-1}$ at 95 $W\ kg^{-1}$ 32.5 $W\ h\ kg^{-1}$ at 1.8 $kW\ kg^{-1}$	42
NiO/GR//HPNCNT	1200	270	32 $W\ h\ kg^{-1}$ at 700 $W\ kg^{-1}$ 17 $W\ h\ kg^{-1}$ at 42 $kW\ kg^{-1}$	43
β-$Ni(OH)_2$/Ni-foam//AC	790.3 $C\ g^{-1}$	261.8 $C\ g^{-1}$	36.2 $W\ h\ kg^{-1}$ at 100.6 $W\ kg^{-1}$ 10.5 $W\ h\ kg^{-1}$ at 0.7 $kW\ kg^{-1}$	44
CoO@ppy//AC	2223	-	43.5$W\ h\ kg^{-1}$ at 87.5$W\ kg^{-1}$ 11.8 $W\ h\ kg^{-1}$ at 5.5 $kW\ kg^{-1}$	45
$NiCo_2O_4$/GR//HFAC	650	550	48$W\ h\ kg^{-1}$ at 230$W\ kg^{-1}$ 28 $W\ h\ kg^{-1}$ at 1.9 $kW\ kg^{-1}$	19
Co_3O_4/rGO//AC	636	210	35.7$W\ h\ kg^{-1}$ at 225$W\ kg^{-1}$ 30.2 $W\ h\ kg^{-1}$ at 3.7 $kW\ kg^{-1}$	46
$Ni(OH)_2$/GR//porous GR	1735	245	77.8$W\ h\ kg^{-1}$ at 174.7$W\ kg^{-1}$ 13.5 $W\ h\ kg^{-1}$ at 15.2 $kW\ kg^{-1}$	47
$NiCo_2O_4$/GR//AC	618	171	19.5$W\ h\ kg^{-1}$ at 150$W\ kg^{-1}$ 7.5$W\ h\ kg^{-1}$ at 5.6 $kW\ kg^{-1}$	48
Co_3O_4//Carbon	504	272	36$W\ h\ kg^{-1}$ at 1600$W\ kg^{-1}$ 15.4$W\ h\ kg^{-1}$ at 7.9$kW\ kg^{-1}$	49
o-CNT/$Ni(OH)_2$//rGO	1368	-	35.24$W\ h\ kg^{-1}$ at 1807$W\ kg^{-1}$ 26.24$W\ h\ kg^{-1}$ at 27$kW\ kg^{-1}$	50
meso-NiO/Ni-3//CNCs	2735	226	19.1 $W\ h\ kg^{-1}$ at 700 $W\ kg^{-1}$ 11.7 $W\ h\ kg^{-1}$ at 13.6 $kW\ kg^{-1}$	51
$ZnCo_2O_4$/$NiMoO_4$//AC	1480.5	-	48.6 $W\ h\ kg^{-1}$ at 112.7 $W\ kg^{-1}$ 13 $W\ h\ kg^{-1}$ at 2.8 $kW\ kg^{-1}$	52
$NiCo_2O_4$-rGO//rGO	1185	-	33.5 $W\ h\ kg^{-1}$ at 523.2 $W\ kg^{-1}$ 19.8 $W\ h\ kg^{-1}$ at 8.9 $kW\ kg^{-1}$	53
$ZnCo_2O_4$/NG//AC	301.8	208	28.3 $W\ h\ kg^{-1}$ at 500 $W\ kg^{-1}$	54

			15.1 W h kg^{-1} at 9.9 kW kg^{-1}	
Co_3O_4//AC	1087.3	140	32.8 W h kg^{-1} at 752 W kg^{-1} 20.3 W h kg^{-1} at 11.2 kW kg^{-1}	55
Co_9S_8@Ni(OH)$_2$//AC	149.5mAh g^{-1}	-	31.35 W h kg^{-1} at 252.8 W kg^{-1} 12.5 W h kg^{-1} at 2.5 kW kg^{-1}	56
$NiCo_2O_4$/NSCS//NGN/CNTs	733	-	47.65 W h kg^{-1} at 536 W kg^{-1} 28.94 W h kg^{-1} at 13.0 kW kg^{-1}	57
Carbon black/$NiCo_2O_4$//AC	1215	173.6	33.7 W h kg^{-1} at 150.1 W kg^{-1} 15.1 W h kg^{-1} at 12.2 kW kg^{-1}	58
C/$CoNi_3O_4$//AC	855.5	129.8	29.1 W h kg^{-1} at 130.4 W kg^{-1} 19.2 W h kg^{-1} at 13.0 kW kg^{-1}	59

Notes and references

1 L. Hu, J. Hou, Y. Ma, H. Li and T. Zhai, *J. Mater. Chem. A*, 2016, **4**, 15006-15014.

2 C. Chen, D. Yu, G. Zhao, B. Du, W. Tang, L. Sun, Y. Sun, F. Besenbacher and M. Yu, *Nano Energy*, 2016, **27**, 377-389.

3 N. Mao, H. Wang, Y. Sui, Y. Cui, J. Pokrzywinski, J. Shi, W. Liu, S. Chen, X. Wang and D. Mitlin, *Nano Res.*, 2017, **10**, 1767-1783.

4 X. Wei, S. Wan, X. Jiang, Z. Wang and S. Gao, *ACS Appl. Mater. Interfaces*, 2015, **7**, 22238-22245.

5 X. Wu, D. Yang, C. Wang, Y. Jiang, T. Wei and Z. Fan, *Carbon*, 2015, **92**,

26-30.

6 C. Long, D. Qi, T. Wei, J. Yan, L. Jiang and Z. Fan, *Adv. Funct. Mater.*, 2014, **24**, 3953-3961.

7 S. Song, F. Ma, G. Wu, D. Ma, W. Geng and J. Wan, *J. Mater. Chem. A*, 2015, **3**, 18154-18162.

8 W. Qian, J. Zhu, Y. Zhang, X. Wu and F. Yan, *Small*, 2015, **11**, 4959-4969.

9 L. Wan, J. Wang, L. Xie, Y. Sun and K. Li, *ACS Appl. Mater. Interfaces*, 2014, **6**, 15583-15596.

10 Q. Liang, L. Ye, Z. H. Huang, Q. Xu, Y. Bai, F. Kang and Q. H. Yang, *Nanoscale*, 2014, **6**, 13831-13837.

11 P. Cheng, T. Li, H. Yu, L. Zhi, Z. Liu and Z. Lei, *J. Phys. Chem. C*, 2016, **120**, 2079-2086.

12 Y. Li, G. Wang, T. Wei, Z. Fan and P. Yan, *Nano Energy*, 2016, **19**, 165-175.

13 Z. Xu, X. Zhuang, C. Yang, J. Cao, Z. Yao, Y. Tang, J. Jiang, D. Wu and X. Feng, *Adv. Mater.*, 2016, **28**, 1981-1987.

14 W. Qian, F. Sun, Y. Xu, L. Qiu, C. Liu, S. Wang and F. Yan, *Energy Environ. Sci.*, 2014, **7**, 379-386.

15 X. Zhang, Y. Jiao, L. Sun, L. Wang, A. Wu, H. Yan, M. Meng, C. Tian, B. Jiang and H. Fu, *Nanoscale*, 2016, **8**, 2418-2427.

16 Y.-Q. Zhao, M. Lu, P.-Y. Tao, Y.-J. Zhang, X.-T. Gong, Z. Yang, G.-Q. Zhang and H.-L. Li, *J. Power Sources*, 2016, **307**, 391-400.

17 J. Xu, Z. Tan, W. Zeng, G. Chen, S. Wu, Y. Zhao, K. Ni, Z. Tao, M. Ikram, H. Ji and Y. Zhu, *Adv. Mater.*, 2016, **28**, 5222-5228.

18 J. Zhu, D. Xu, W. Qian, J. Zhang and F. Yan, *Small*, 2016, **12**, 1935-1944.

19 Z. Li, Z. Xu, H. Wang, J. Ding, B. Zahiri, C. M. B. Holt, X. Tan and D. Mitlin, *Energy Environ. Sci.*, 2014, **7**, 1708-1718.

20 L. Jiang, L. Sheng, X. Chen, T. Wei and Z. Fan, *J. Mater. Chem. A*, 2016, **4**, 11388-11396.

21 L.-N. Han, X. Wei, Q.-C. Zhu, S.-M. Xu, K.-X. Wang and J.-S. Chen, *J. Mater. Chem. A*, 2016, **4**, 16698-16705.

22 P. Yu, Z. Zhang, L. Zheng, F. Teng, L. Hu and X. Fang, *Adv. Energy Mater.*, 2016, **6**, 1601111.

23 Y. Zhang, X. Liu, S. Wang, S. Dou and L. Li, *J. Mater. Chem. A*, 2016, **4**, 10869-10877.

24 X.-L. Su, M.-Y. Cheng, L. Fu, J.-H. Yang, X.-C. Zheng and X.-X. Guan, *J. Power Sources*, 2017, **362**, 27-38.

25 H. Ma, C. Li, M. Zhang, J.-D. Hong and G. Shi, *J. Mater. Chem. A*, 2017, **5**, 17040-17047.

26 Y. Boyjoo, Y. Cheng, H. Zhong, H. Tian, J. Pan, V. K. Pareek, S. P. Jiang, J.-F. Lamonier, M. Jaroniec and J. Liu, *Carbon*, 2017, **116**, 490-499.

27 C. Wang, Y. Xiong, H. Wang, C. Jin and Q. Sun, *J. Mater. Chem. A*, 2017, **5**, 15759-15770.

28 J. Shao, F. Ma, G. Wu, C. Dai, W. Geng, S. Song and J. Wan, *Chem. Eng. J.*, 2017, **321**, 301-313.

29 Y. Liu, B. Huang, X. Lin and Z. Xie, *J. Mater. Chem. A*, 2017, **5**, 13009-13018.

30 T. Ouyang, K. Cheng, Y. Gao, S. Kong, K. Ye, G. Wang and D. Cao, *J. Mater. Chem. A*, 2016, **4**, 9832-9843.

31 M. Genovese and K. Lian, *J. Mater. Chem. A*, 2017, **5**, 3939-3947.

32 L. Zhu, F. Shen, R. L. Smith, L. Yan, L. Li and X. Qi, *Chem. Eng. J.*, 2017, **316**, 770-777.

33 X. Wei, Y. Li and S. Gao, *J. Mater. Chem. A*, 2017, **5**, 181-188.

34 F. Ma, D. Ma, G. Wu, W. Geng, J. Shao, S. Song, J. Wan and J. Qiu, *Chem. Commun.*, 2016, **52**, 6673-6676.

35 Y. Zhang, S. Liu, X. Zheng, X. Wang, Y. Xu, H. Tang, F. Kang, Q.-H. Yang and J. Luo, *Adv. Funct. Mater.*, 2017, **27**, 1604687.

36 Y. Cui, H. Wang, X. Xu, Y. Lv, J. Shi, W. Liu, S. Chen and X. Wang, *Sustainable Energy Fuels*, 2018, **2**, 381-391.

37 Z. H. Huang, T. Y. Liu, Y. Song, Y. Li and X. X. Liu, *Nanoscale*, 2017, **9**, 13119-13127.

38 X. Wang, C. Yan, A. Sumboja and P. S. Lee, *Nano Energy*, 2014, **3**, 119-126.

39 Y. Zhang, B. Wang, F. Liu, J. Cheng, X. Zhang and L. Zhang, *Nano Energy*, 2016, **27**, 627-637.

40 Y. Zhu, Z. Wu, M. Jing, H. Hou, Y. Yang, Y. Zhang, X. Yang, W. Song, X. Jia and X. Ji, *J. Mater. Chem. A*, 2015, **3**, 866-877.

41 L. Shen, L. Yu, H. B. Wu, X. Y. Yu, X. Zhang and X. W. Lou, *Nat. Commun.*, 2015, **6**, 6694.

42 Z. Tang, C. Tang and H. Gong, *Adv. Funct. Mater.*, 2012, **22**, 1272-1278.

43 H. Wang, H. Yi, X. Chen and X. Wang, *J. Mater. Chem. A*, 2014, **2**, 3223-3230.

44 J. Huang, P. Xu, D. Cao, X. Zhou, S. Yang, Y. Li and G. Wang, *J. Power Sources*, 2014, **246**, 371-376.

45 C. Zhou, Y. Zhang, Y. Li and J. Liu, *Nano Lett.*, 2013, **13**, 2078-2085.

46 L.-J. Xie, J.-F. Wu, C.-M. Chen, C.-M. Zhang, L. Wan, J.-L. Wang, Q.-Q. Kong, C.-X. Lv, K.-X. Li and G.-H. Sun, *J. Power Sources*, 2013, **242**, 148-156.

47 J. Yan, Z. Fan, W. Sun, G. Ning, T. Wei, Q. Zhang, R. Zhang, L. Zhi and F. Wei, *Adv. Funct. Mater.*, 2012, **22**, 2632-2641.

48 H. Wang, C. M. B. Holt, Z. Li, X. Tan, B. S. Amirkhiz, Z. Xu, B. C. Olsen, T. Stephenson and D. Mitlin, *Nano Res.*, 2012, **5**, 605-617.

49 R. R. Salunkhe, J. Tang, Y. Kamachi, T. Nakato, J. H. Kim, and Y. Yamauchi, ACS Nano, 2015, 9, 6288–6296.

50 R. R. Salunkhe, J. Lin, V. Malgras, S. X. Dou, J. H. Kim and Y. Yamauchi, *Nano Energy*, 2015, **11**, 211-218.

51 H. Lai, Q. Wu, J. Zhao, L. Shang, H. Li, R. Che, Z. Lyu, J. Xiong, L. Yang, X. Wang and Z. Hu, *Energy Environ. Sci.*, 2016, **9**, 2053-2060.

52 J. Hong, Y.-W. Lee, D. Ahn, S. Pak, J. Lee, A. R. Jang, S. Lee, B. Hou, Y. Cho, S. M. Morris, H. S. Shin, S. Cha, J. I. Sohn and J. M. Kim, *Nano Energy*, 2017, **39**, 337-345.

53 S. A.-Rubaye, R. Rajagopalan, S. X. Dou and Z. Cheng, *J. Mater. Chem. A*,

2017, **5**, 18989-18997.

54 X. Ma, P. Zhang, Y. Zhao, Y. Liu, J. Li, J. Y. Zhou, X. Pan and E. Xie, *Chem. Eng. J.*, 2017, **327**, 1000-1010.

55 Z. Xiao, L. Fan, B. Xu, S. Zhang, W. Kang, Z. Kang, H. Lin, X. Liu, S. Zhang and D. Sun, *ACS Appl. Mater. Interfaces*, 2017, **9**, 41827-41836.

56 F. Zhu, M. Yan, Y. Liu, H. Shen, Y. Lei and W. Shi, *J. Mater. Chem. A*, 2017, **5**, 22782-22789.

57 H. Tong, S. Yue, L. Lu, F. Jin, Q. Han, X. Zhang and J. Liu, *Nanoscale*, 2017, **9**, 16826-16835.

58 D. Zha, Y. Fu, X. Gao, L. Zhang and X. Wang, *Electrochim. Acta*, 2017, **257**, 494-503.

59 J. Zhu, J. Jiang, Z. Sun, J. Luo, Z. Fan, X. Huang, H. Zhang and T. Yu, *Small*, 2014, **10**, 2937-2945.